CHIN. PHYS. LETT. Vol. 30, No. 4 (2013) 047301

Characteristics of an Indium-Rich InGaN p–n Junction Grown on a Strain-Relaxed InGaN Buffer Layer *

YANG Lian-Hong(杨莲红)**, ZHANG Bao-Hua(张保花), GUO Fu-Qiang(郭福强)

Xinjiang Laboratory of Phase Transitions and Microstructures of Condensed Matter, Yili Normal University, Yining 835000

Department of Physics, Changji College, Changji 831100

(Received 25 October 2012)

An indium-rich InGaN p–n junction is grown on a strain-relaxed InGaN buffer layer. The results show that the n-InGaN is grown coherently on the buffer layer but the p-InGaN layer exhibits a partial strain relaxation. The fabricated InGaN p–n junction has a low reverse leakage current density on the order of 10^{-8} A/cm^2 within the measured voltage range, and exhibits a wide spectral response due to the presence of band tail states or deep level states which origin from indium composition fluctuation or various defects. The measured peak responsivity at 438 nm is 31 mA/W at zero bias and reaches 118 mA/W at 3 V reverse bias. In addition, the Raman spectra of the p- and n-type InGaN alloys are also analyzed.

PACS: 73.40.Kp, 85.60.Bt, 81.05.Ea DOI: 10.1088/0256-307X/30/4/047301

InGaN films have been widely used as active layers for blue light-emitting diodes (LEDs) and laser diodes (LDs).[1–3] Recently, indium-rich InGaN alloys have attracted much attention because of their potential applications in the fields of green LEDs and LDs,[4] solar cells,[5–8] and photodetectors,[9,10] thanks to their tunable band gap ranging from infrared to ultraviolet. However, the growth of indium-rich InGaN films, commonly on GaN substrates, suffers from serious problems owing to the large lattice mismatch and growth temperature mismatch between InGaN and GaN, which will induce high strain and may result in dislocations, phase separation, and V-pits.[11,12] Meanwhile, the p-type doping of indium-rich InGaN alloys faces a larger challenge because of the low p-doping efficiency and a high n-type background carrier concentration as well as phase separation.[13]

In this work, a fully strain-relaxed InGaN buffer layer was induced in order to achieve an indium-rich InGaN p–n junction with a full strain or less strain relaxation. The indium contents in the n-type layer and in the buffer layer are the same, and thus the n-type layer can grow coherently onto buffer. Structural and photoelectric properties of the indium-rich InGaN p–n junction are investigated by using x-ray diffraction (XRD), Raman, and photocurrent response measurements, respectively.

The indium-rich InGaN structure was grown on a 30-nm-thick GaN nucleation layer/(0001) sapphire substrate by metal-organic chemical vapor deposition (MOCVD). Following a 1.0-μm-thick high-temperature unintentionally doped GaN layer, a 500-nm-thick unintentionally doped InGaN buffer layer and a Si-doped InGaN layer with the same thickness as the buffer layer were grown in sequence under the same growth conditions. Then, a 20-nm-thick InGaN compositional grading layer and a 100-nm-thick p-InGaN layer were grown at 700℃. The Si doping concentrations for the n-InGaN is 5×10^{18} cm^{-3}. The Mg doping concentration is 2×10^{17} cm^{-3} for the p-InGaN layer. For current-voltage (I–V) measurements, the n-InGaN ohmic contact was formed by depositing Ti/Al/Ni/Au (20/100/30/100 nm) metal layers using e-beam evaporation after the mesa with a size of 800×800 μm^2 was defined via photolithography and dry etching, and the p-InGaN ohmic contact with finger electrode structure was formed by depositing Ni/Au (30/100 nm) layers followed by an annealing treatment at 500℃ for 5 min in a flowing O_2 atmosphere.

Figure 1 shows the $\omega/2\theta$ scan of the symmetric (0002) reflection of the InGaN p–n junction. According to the sample structure, the strongest diffraction peak at the angle of 17.27° originates from the GaN layer, and two other diffraction peaks correspond to the InGaN p–n junction. The diffraction peak on the low-angle side is confirmed to be from the contributions of the n-InGaN and InGaN buffer layers which are nominally of the same indium content, and the other peak with stronger diffraction strength is from the p-InGaN layer which was designed to be of lower indium content due to the difficulty of p-doping of high-indium-content InGaN alloys. The full width at half maximums (FWHMs) of the (0002) reflection peaks of the p-InGaN and n-InGaN layers are 576 and 871 arcsec, respectively. To determine the in-plane and out-of-plane lattice constants (a and c, respectively) and indium content of each layer, we also

*Supported by the Opening Project of Xinjiang Laboratory of Phase Transitions and Microstructures of Condensed Matters (Nos XJDX0912-2012-03, XJDX0912-2012-02), the Project of Changji Collge (Nos 2011YJYB001, 2011YJYB006).

**Corresponding author. Email: xjylh01@hotmail.com

© 2013 Chinese Physical Society and IOP Publishing Ltd

recorded the asymmetric (105) reflection of the InGaN sample as shown in Fig. 2, exhibiting the FWHMs of the ω–θ curves of 1083 and 1139 arcsec, respectively, for the p-InGaN and n-InGaN layers. From Figs. 1 and 2, the n-InGaN layer and the InGaN buffer exhibit completely identical lattice constants, indicating the coherent growth of the n-InGaN layer on the InGaN buffer. The indium content and lattice parameters of each layer can be determined using elastic strain theory with an assumption that Vegard's law is valid in the InGaN alloy. The calculated a and c of the buffer and n-InGaN layers are 0.3409 nm and 0.5464 nm, respectively, and indium content is 36.9%. For the p-InGaN, a and c are 0.3363 nm and 0.5368 nm, respectively, and indium content is 21.9%. The calculated strain in the p-InGaN is 0.0298, showing a partial relaxation.

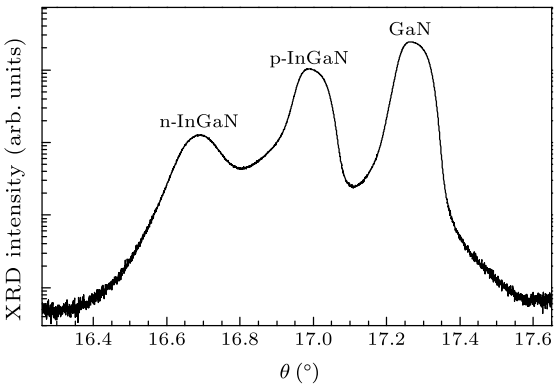

Fig. 1. Characteristics of $\omega/2\theta$ scan of the symmetric (0002) reflection of the InGaN p–n junction.

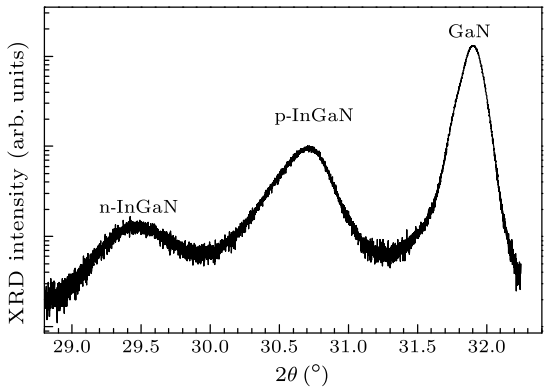

Fig. 2. Asymmetric (105) reflection of the InGaN p–n junction.

Figure 3 shows the room-temperature Raman spectra of the InGaN p–n junction recorded in the $z(xx)z$ back scattering geometry by using the 514.5-nm line of an Ar^+ laser. In this configuration, only the E_2 and the A_1(LO) modes are allowed. The top spectrum is from the p-InGaN layer, and the bottom one is from the n-InGaN layer. The Raman spectrum of the n-InGaN was measured after etching off the p-InGaN layer. From Fig. 3, we can observe that the p-InGaN spectrum exhibits a strong A_1(LO) peak at 704 cm^{-1} and a weak and broadening E_2 peak with the center at 548 cm^{-1}, whilst the n-InGaN with a higher indium composition exhibits a weaker A_1(LO) peak at 647 cm^{-1} but a more obvious E_2 mode with the center at 511 cm^{-1}. The weaker A_1(LO) peak in the n-InGaN can be attributed to a high-free carrier concentration of the order of 10^{18} cm^{-3} in the film. Since the high-concentration free carriers are easy to form plasmon waves that interact and, in turn, damp the LO phonons.[14] It can also be observed from the p-InGaN spectrum that the A_1(LO) peak exhibits a low-frequency tail extending down to about 650 cm^{-1}, which is possibly related to the InGaN compositional grading layer in our sample. In Ref. [15], this frequency tail was assigned to disorder-activated modes which become Raman active due to the relaxation of wave-vector conservation caused by the presence of structural defects and the random cation distribution in the alloy because this position coincides with a region with a high phonon density of states in GaN.

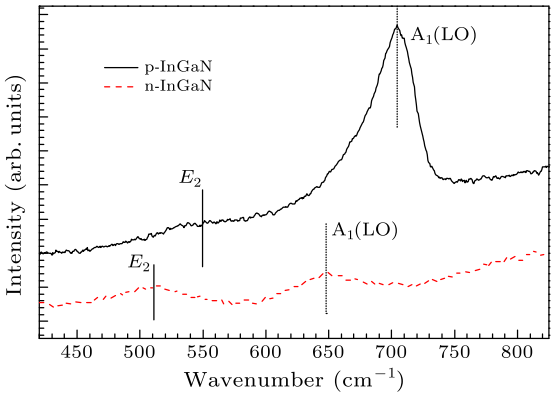

Fig. 3. Raman spectra of the p-type and n-type InGaN alloys recorded in the $z(xx)z$ back scattering geometry.

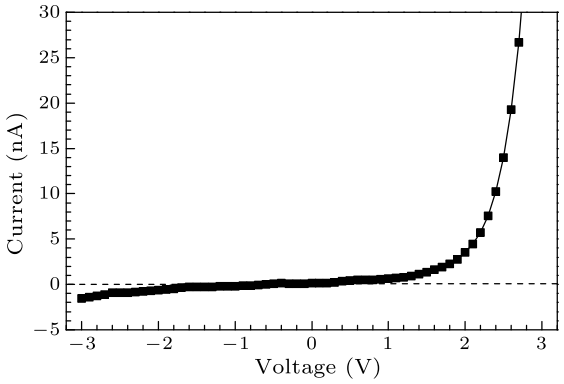

Fig. 4. The I–V characteristics of the InGaN p–n junction.

Figure 4 shows the I–V characteristic of the InGaN p–n junction. It can be seen that the sample, in general, exhibits a good p–n junction behavior, although the reverse leakage current increases gradually with increasing reverse bias due to the presence of a number of recombination centers in the indium-rich

InGaN sample. It was well known that the depletion region in the p–n junction becomes wider with increasing reverse bias, and hence the generated current from recombination centers in the depletion region becomes unsaturated under reverse bias. However, reverse leakage current density in the measured voltage range, in general, is very low with the order of 10^{-8} A/cm^2 in the high-defect-density indium-rich InGaN material system.

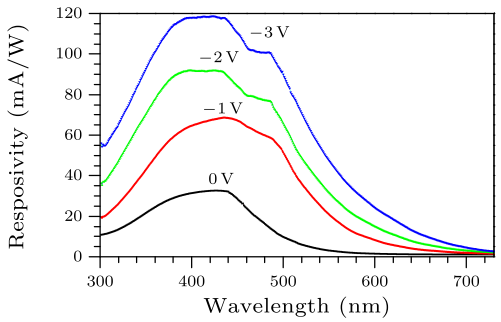

Fig. 5. Photocurrent response of the InGaN p–n junction at various reverse bias voltages.

Figure 5 shows the photocurrent response of the InGaN p–n junction at various reverse bias voltages. All of the photocurrent spectra show a wide range of wavelength response and exhibit no sharp cutoff. The maximum responsivity occurs at around 438 nm, corresponding to the band edge of p-InGaN. With increasing reverse bias, another cutoff occurs at around 490 nm, corresponding to the band edge of n-InGaN. At zero bias or low bias, the depletion region prefers to expand toward the p-InGaN layer due to the lower p-type doping concentration, and thus only a cutoff corresponding to the band edge of the p-InGaN can be observed. At a short wavelength direction of the response spectra, the responsivity drops rather than a flat response. This phenomenon can be attributed to stronger absorption at the surface of the p-InGaN due to a higher absorption coefficient at shorter wavelength. It is well known that InGaN alloys have a very high surface state density and hence remain a deep non-depleted region at the surface.[16] Thus, only a few photons are absorbed in the depletion region and generate photocurrent at short wavelengths. At long wavelength direction, a wide range of photocurrent response below band edge of the n-InGaN occurs. This photocurrent response below band edge is attributed to the presence of a number of band tail states or deep level states in the indium-rich InGaN alloys. The origin of the band tail states could be assigned to various causes, such as indium composition fluctuation which has been commonly observed in indium-rich InGaN alloys,[17] shallow donors such as nitrogen vacancies and oxygen impurities, inhomogeneous lattice deformation, etc. The deep level states are likely associated with the high density of dislocations. The transition process from valence band to shallow band tail states or from the deep level states to the conduction band can happen even if the energy of the illuminated photons is below band edge of the n-InGaN. These processes can also generate photocurrent assisted by the applied or build-in electric fields and result in the wide response below the band edge of the n-InGaN. The measured peak responsivity at 438 nm is 31 mA/W at zero bias and reaches 118 mA/W at 3 V reverse bias.

In summary, an indium-rich InGaN p–n junction grown on a strain-relaxed InGaN buffer layer has been investigated. The XRD measurement shows that the n-InGaN was grown coherently on the buffer layer but the p-InGaN layer exhibits a partial strain relaxation. Raman spectra show that A_1 (LO) peak and E_2 peak present different behaviors in the p-InGaN and n-InGaN alloys due to the discrepancies of indium content and carrier concentration. The fabricated InGaN p–n junction has a low reverse leakage current density in the measured voltage range, and exhibits a wide spectral response due to the presence of band tail states or deep level states.

References

[1] Wierer J J Krames M R, Epler J E, Gardner N F, Craford M G, Wendt J R, Simmons J A and Sigalas M M 2004 *Appl. Phys. Lett.* **84** 3885
[2] Nakamura S 1998 *Science* **281** 956
[3] Narukawa Y, Kawakami Y, Funato M and Fujita S 1997 *Appl. Phys. Lett.* **70** 981
[4] Yang Y, Cao X A and Yan C H 2009 *Appl. Phys. Lett.* **94** 041117
[5] Dahal R, Li J, Aryal K, Lin J Y and Jiang H X 2010 *Appl. Phys. Lett.* **97** 073115
[6] Zhang X B, Wang X L, Xiao H L, Yang C B, Hou Q F, Yin H B, Chen H and Wang Z G 2011 *Chin. Phys.* B **20** 028402
[7] Cai X M, Zeng S W and Zhang B P 2009 *Appl. Phys. Lett.* **95** 173504
[8] Xue J J, Chen D J, Liu B, Xie Z L, Jiang R L, Zhang R and Zheng Y D 2009 *Chin. Phys. Lett.* **26** 098102
[9] Sang L W, Liao M Y, Koide Y and Sumiya M 2011 *Appl. Phys. Lett.* **98** 103502
[10] Chen D J, Liu B, Lu H, Xie Z L, Zhang R and Zheng Y D 2009 *IEEE Electron Device Lett.* **30** 605
[11] Singh R, Doppalapudi D, Moustakas T D and Romano L T 1997 *Appl. Phys. Lett.* **70** 1089
[12] Fischer A M, Wu Z, Sun K, Wei Q Y, Huang Y, Senda R, Iida D, Iwaya M, Amano H and Ponce F A 2009 *Appl. Phys. Express* **2** 041002
[13] Sang L, Takeguchi M, Lee W, Nakayama Y, Lozach M, Sekiguchi T and Sumiya M 2010 *Appl. Phys. Express* **3** 111004
[14] Alexson D, Bergman L, Nemanich R J, Dutta M, Stroscio M A, Parker C A, Bedair S M, E I-Masry N A and Adar F 2001 *J. Appl. Phys.* **89** 798
[15] Hernandez S, Cusco R, Pastor D, Artus L, O'Donnell K P, Martin R W, Watson I M, Nanishi Y and Calleja E 2005 *J. Appl. Phys.* **98** 013511
[16] Chen D J, Huang Y, Liu B, Xie Z L, Zhang R, Zheng Y D, Wei Y and Narayanamurti V 2009 *J. Appl. Phys.* **105** 063714
[17] Lai K Y, Lin G J, Lai Y L, Chen Y F and He J H 2010 *Appl. Phys. Lett.* **96** 081103